ISSN 0967-859X
THE SOCIETY FOR EARTHQUAKE AND CIVIL ENGINEERING DYNAMICS

NEWSLETTER

Volume 28 No 3
December 2017

In this issue

Brougher Mountain Tower – Dynamic Response and Damper Design

John Rees
COWI UK Ltd, Chipping Sodbury, UK

Introduction

Early in 2010, reports were received of excessive and uncharacteristic vibrations at Arqiva's tower at Brougher Mountain in Northern Ireland. The vibrations followed the installation of a new digital TV cantilever antenna and a modest extension to the tower. The paper will explain the investigation undertaken by COWI (formerly Flint & Neill) and the development of a solution to mitigate the vibrations.

Investigation

Brougher Mountain Tower is a conventional four-legged steel lattice tower. The face width of the tower is 7.389 m at ground level, tapering to 1.600 m at the 46 m level and then remaining constant up to the top of the tower at the 53.619 m level. The overall height is 64 m, which includes a 10.5 m tall cantilever spine supporting an array of 8 tiers of four panels of UHF antennas. The spine is 0.640 m square and the addition of panel antennas gives a typical projected width of 1.25 m.

Based on video footage, it was clear that the tower was oscillating in its fundamental mode. Reports from site suggested that the motion was cross-wind. The vibration amplitude was more difficult to judge, as there was no fixed

Editor's note: On 22nd February 2017, SECED and the Wind Engineering Society (WES) jointly hosted an event at the Institution of Civil Engineers. The entire last issue was dedicated to a paper summarising the first talk by presenters Roy Crielaard and William Algaard, with co-author William Whitby (Arup). This article is a summary of the second talk, provided by John Rees (COWI UK Ltd).

reference point. However, it was estimated that the vibration amplitude did not exceed 200 mm. There was a limited amount of information on the wind speed and direction associated with the video records. Despite this, it was considered that cross-wind response under the action of vortex shedding was the most likely explanation. Therefore, the initial investigation focussed on this mechanism.

A finite element model of the tower was generated and a modal analysis was carried out. The tower's fundamental frequency was calculated as 1.29 Hz, which was close to that estimated from video footage. Resonant cross-wind response may occur at any wind speed where the vortex-shedding frequency matches a natural frequency of the tower. These 'critical' wind-speeds (V_{cr}) and are related to a structure's natural frequency by the following expression:

$$V_{cr} = \frac{f_n D_z}{S_t} \quad (1)$$

where f_n is the frequency (in Hz) of mode n, D_z is the diameter or cross-wind width of the bluff body (in m) and S_t is the Strouhal number (non-dimensional).

The construction of the cantilever antenna was such that it could not be idealised as a circular or square cross-section. However, it was felt that these two idealisations would provide boundaries to the actual behaviour. Values of Strouhal number of 0.2 and 0.15 were adopted for circular and square idealisations, respectively, and critical wind speeds were calculated for the first four modes of vibration, as shown in Table 1.

Vortex shedding is usually considered up to 1.3 times the hourly mean wind speed at the height of the antenna (V_z), to account for gusts sustained long enough for vortices to correlate and response to build up. For the Brougher Mountain site, $1.3V_z$ was calculated as 72 m/s. This meant the first four modes needed to be considered if the antenna behaved like a circular cross-section and the first three modes if it behaved like a square. However, the risk of vortex shedding diminishes at high Scruton numbers.

This characteristic was assessed for mode 1 by application of BS EN 1991-1-4: Annex E: Approach 2 (based on the work of Vickery & Basu, 1983). Calculated responses were produced assuming both a circular and square cross section for a range of Scruton numbers (in effect by varying the damping). The results are plotted in Figure 1 and include the observed response (together with error bars to represent an estimated ±50% variation in structural damping and response).

The Scruton Number is defined as:

$$S_c = \frac{2\delta_s m_e}{\rho_a D_z^2} \quad (2a)$$

where:

$$m_e = \frac{\int_0^h m(z)\mu^2(z)dz}{\int_{z1}^{z2} \mu^2(z)dz} \quad (2b)$$

Table 1: Critical wind speed calculations for first four modes of vibration.

Mode No.	Frequency (Hz)	Cross-section	V_{cr} (m/s)
1	1.29	Square	8.1
		Circular	10.7
2	3.86	Square	24.1
		Circular	32.1
3	6.54	Square	40.9
		Circular	54.5
4	9.95	Square	62.2
		Circular	(82.9)

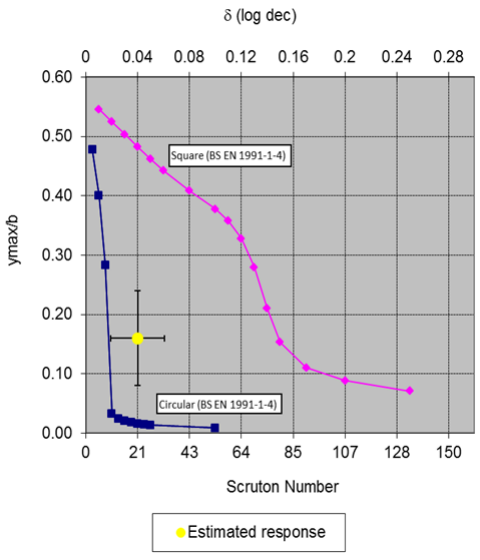

Figure 1: Calculated responses to BS EN 1991-1-4, assuming circular and square cross-section.

Table 2: Measured vs calculated frequencies.

Mode No.	Measured frequency (Hz)	Calculated frequency (Hz)	% difference
1	1.28	1.29	0.8%
2	3.2	3.86	20.6%
3	5.0	6.54	30.8%

where δ_s is the logarithmic decrement of structural damping, ρ_a is the density of air, $m(z)$ is the mass per unit length, $\mu(z)$ is the mode shape and $z1$ and $z2$ are the lower and upper limits of the bluff body (i.e. the antenna), respectively.

Thus the initial investigation indicated that the behaviour of the antenna was closer to that of a cylinder than a square. Furthermore, responses in modes 3 and 4 were most unlikely as the associated Scruton numbers were too large. The plot also shows that introduction of additional damping to supplement the structural damping could effectively suppress responses.

Options for a type of damper were debated with Arqiva and quickly narrowed down to hanging chain impact dampers. Restrictions on land around the tower eliminated ground based dampers, connected to the tower with lightweight guys. Chain dampers offered a low tech and minimal maintenance solution with which Arqiva had considerable experience (they had been installed on Belmont and Winter Hill masts in the 1970s and performed reliably ever since).

A preliminary damper design was prepared to establish feasibility. Practical constraints meant that the damper for mode 1 was placed just below the cantilever spine and the damper for mode 2 could be located at the base of the parallel tower section if required.

In order to design a damping system, it is necessary to know the natural frequency and expected amplitudes of vibration of each mode under consideration. It was considered that the information available from the video footage was not sufficient and so an instrumentation system was installed to monitor the tower and collect data to inform the design of the damping system.

This consisted of accelerometers at the proposed level of each damper, measuring acceleration in orthogonal horizontal planes, a single anemometer at the 52.4 m level and a temperature probe. Adoption of a single anemometer was a compromise between cost and collection of useful data. Wind from 330° ETN clockwise through to 60° ETN passed through the structure before reaching the anemometer, so data for this range of wind directions was discarded.

Fourier analysis of the data gave a frequency spectrum from which natural frequencies could be identified. Comparison with calculated values, obtained from the finite element (FE) model is given in Table 2. Agreement with mode 1 was good, but agreement with modes 2 and 3 diverged.

The event plot shown in Figure 2 is typical of a period where strong accelerations were observed.

The following characteristics are noted:

- The high amplitude responses last for about 15 minutes;
- The wind direction is 305° ETN and the response of the tower lies on a 25° ETN – 205° ETN axis. So the angle between the wind direction and the vibration axis is ≈80°. This confirms that the response is 'cross-wind'.
- The wind speed throughout the event is ≈8 m/s and this corresponds to the expected critical wind speed for mode 1 vortex shedding response for an antenna whose behaviour is closest to an idealisation of a cylinder.
- The accelerations measured for the two sets of accelerometers are in phase with a ratio of 0.70. This matches the relative modal displacements predicted by the FE model for mode 1.

If it is assumed that the tower's vibration in mode 1 can be approximated as simple harmonic motion, this can be written as $y = A\sin(\omega t)$ where A is amplitude, ω is circular frequency and t is time. If this equation is differentiated twice to give acceleration ($\ddot{y}$) and re-arranged (noting that $\omega = 2\pi f$), the peak amplitude is given by:

$$A = \frac{\ddot{y}}{\omega^2} = \frac{\ddot{y}}{4\pi^2 f^2} \tag{3}$$

The greatest acceleration recorded during the monitoring period was 0.47g at the 52.6 m level and this translates into a peak amplitude of ≈121 mm. The maximum vibration amplitude estimated from video footage was ±200 mm (but without a reference point) so this is considered to represent reasonable correlation.

One unexpected outcome of the monitoring was a high dependence between wind direction and observed vortex shedding response. Large amplitude cross-wind events were found to align with wind from 120° ETN, 210° ETN and 300° ETN (noting that wind from 030° ETN was discarded because of the position of the anemometer). These three directions are at 90° intervals and correspond

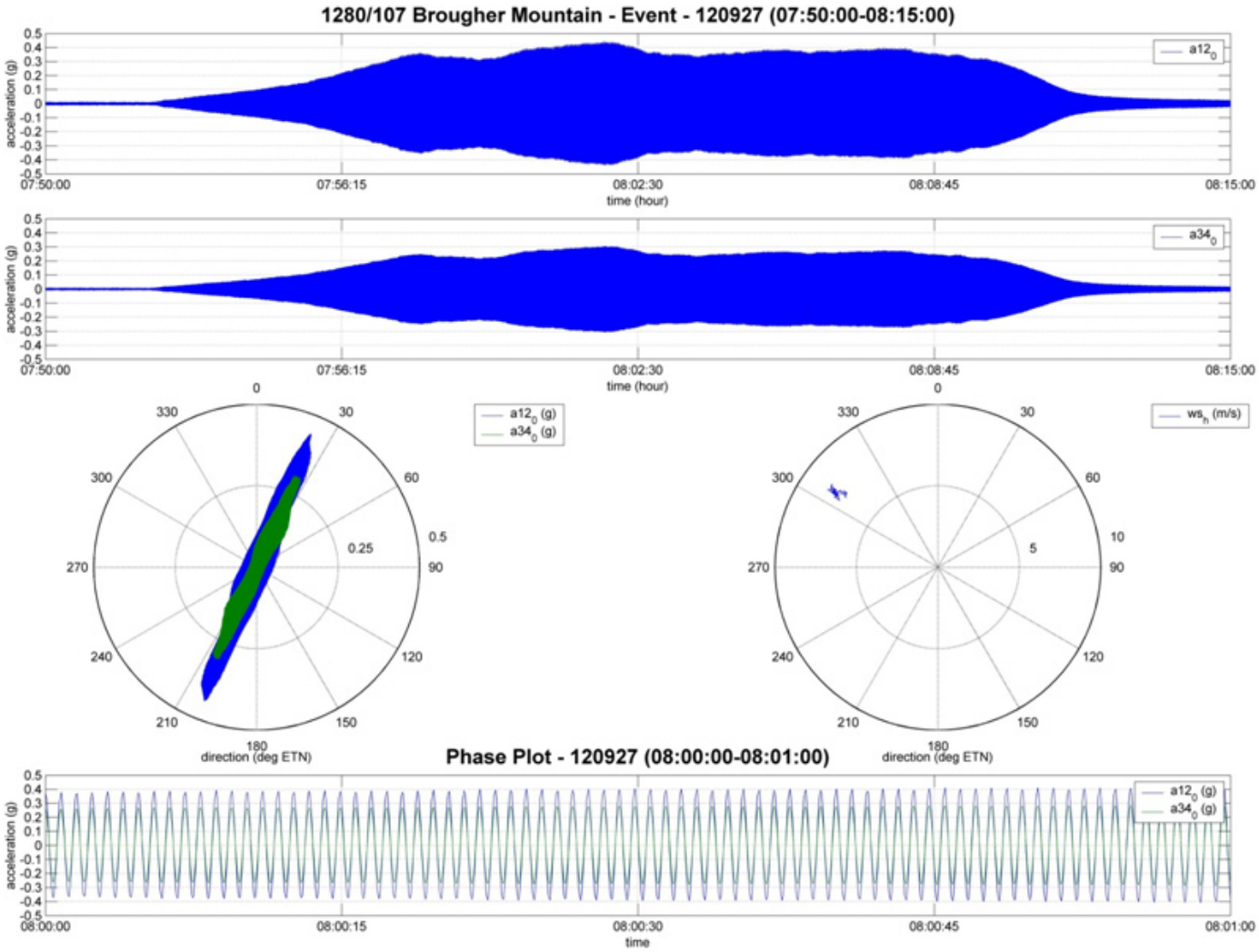

Figure 2: Typical recording of strong accelerations.

approximately to wind on the corner of the tower and the corner of the cantilever antenna.

Based on measured structural frequencies, vortex shedding in mode 2 was expected at a critical wind speed of about 20 m/s. By using filter functions, short duration records at or around the mode 2 critical wind speed were analysed. Some low amplitude mode 2 response was evident, but it was not structurally significant. The plot of wind speed against peak measured acceleration in Figure 3 shows the predominance of mode 1 vortex shedding at or around the expected critical wind speed.

Therefore, the design of a hanging chain impact damper was prepared to suppress vibrations in mode 1. It consisted of a tied bundle of chains suspended centrally from a universal joint within a lined steel tube. The principle by which the damper works is as follows: the chain oscillates out of phase with the motion of the structure and provides a damping force by impacting against the wall of the lined steel tube. The lining provides the required coefficient of restitution (i.e. it ensures that the chain does not bounce too far off the wall of the tube upon impact).

The key parameters in the design of the damper are:

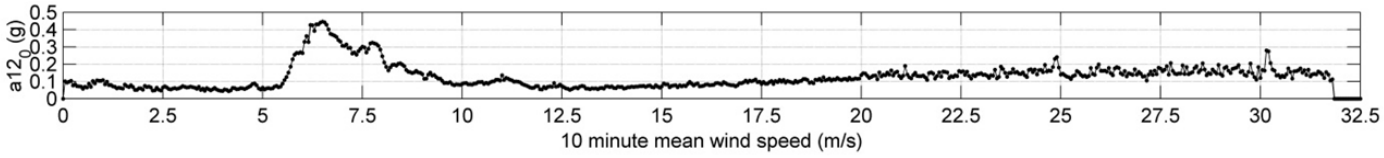

Figure 3: Wind speed vs peak measured acceleration.

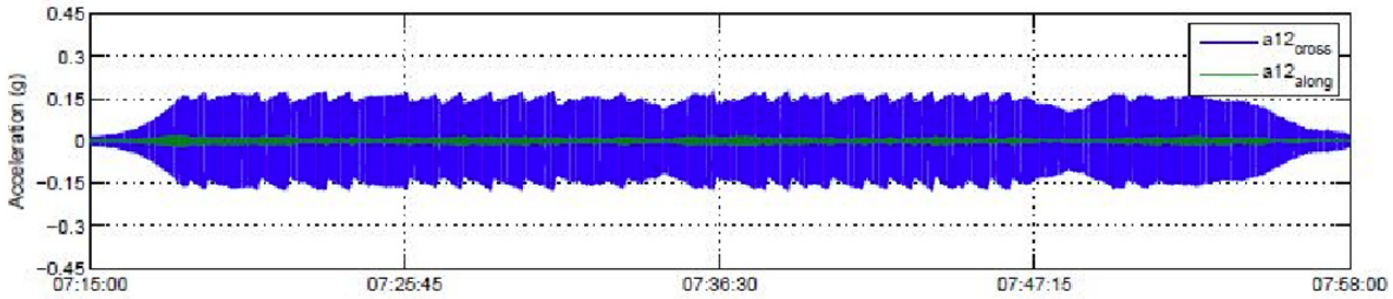

Figure 4: Wind speed vs peak measured acceleration.

- The length of the chain bundle (this determines its natural frequency and this must be set so that it is significantly lower than the frequencies of the structures being damped);
- The mass of the chain bundle (more chain mass results in more damping); and
- The gap between the chain bundle and the tube wall, relative to the damped vibration amplitude of the structure.

An optimal design (in terms of minimum mass of the chain bundle and the efficiency of the damper) could have been produced to dampen the largest vibration amplitudes measured. However, such a damper would not have been effective at smaller vibration amplitudes (i.e. the chain would not have hit the wall of the tube). Instead, it was decided to adopt a heavier chain, and smaller gap between the chain bundle and the tube wall. Whilst this resulted in a less efficient design, it is expected that vibration amplitudes of 30% of the measured peak and above will be damped.

The other key design decision was to set the amount of additional damping provided. As the first figure in the paper shows, a total logarithmic decrement of damping of $\delta = 0.06$ should suppress vortex shedding response by raising the Scruton number to about 30. The structural damping of the tower was set as $\delta = 0.02$ (thus the damper had to augment this, to increase the damping by a factor of three). This is lower than codified values for a tower with angle legs and bracings, and black bolted connections; for example, EN1991-1-4 gives $\delta = 0.05$. However, codified values are provided for use in the calculation of along-wind response at ULS. At lower wind speed events, such as vortex shedding, it is expected that lower levels of damping apply as bolted connections do not slip, so little energy is dissipated through friction.

A further monitoring period followed fabrication and installation, to validate the damper's performance. The event plot shown in Figure 4 shows peak accelerations reduced by about 2/3rds to 0.15g, matching predictions well. The saw-tooth nature of the plot represents a cycle where vortex-shedding response builds until chains hit the tube and provide sufficient damping to suppress it. Response dies down and so the chains no longer hit the tube nor supplement the structure's damping. Vortex-shedding response builds again, until the chains hit the tube and the cycle repeats.

References

Reed, W. H. (2005). Hanging chain impact dampers: a simple method for damping tall flexible structures. *International Research Seminar – Wind Effects on Buildings and Structures*, Ottawa, Canada

Vickery, B. J., & Basu, R. I. (1983). Across-wind vibrations of structures of circular cross-section. Part 1. Development of a mathematical model for two-dimensional conditions. *Journal of Wind Engineering and Industrial Aerodynamics*, **12:** 49–73.

BS EN 1991-1-4: Eurocode 1: Actions on structures. Part 1–4: General actions – wind actions (incorporating corrigenda July 2009 & January 2010).

Base-Isolated Buildings for Controlling Groundborne Vibration: Towards a Performance-Based Design Approach

James P. Talbot
Department of Engineering, University of Cambridge, UK.

Base isolation is well known within the seismic community as a means of protecting buildings from earthquakes. A related technique, also known as base isolation, is known to the noise and vibration community as a means of limiting the disturbance in buildings caused by groundborne vibration, such as that caused by busy roads or railways. The technique has been employed since the 1960s, and across a wide range of buildings. Despite the extensive use of base isolation, there is a significant lack of guidance on all aspects of design, from the selection of bearing type and their location within a building, to questions such as how performance should be evaluated, and the most fundamental question of all: is isolation necessary? This article provides a summary of the author's recent presentation to SECED, which was itself based on a lecture given to ICSV23 [1]. It aims to provide an overview of current design practice, and highlights some of the challenges and future research efforts in this area.

1. Introduction

Since its introduction in the 1960s [2], the use of base isolation to reduce vibration transmission into buildings has grown steadily. There are a number of reasons for this:

- Urban populations have grown considerably, resulting in the expansion of railways, higher density housing and pressure to develop existing 'brown field' sites;
- Environmental standards have risen, in general, and vibration serviceability limits are now a common design requirement for buildings, reflecting the expectations of occupants and the requirements of specialist facilities; and
- Modern buildings are more susceptible to vibration, as more efficient (strength based) design has reduced structural mass, stiffness and damping.

Base-isolated buildings have become commonplace, with examples to be found as offices and apartments, concert halls, cinemas, hospitals and broadcasting studios. See Fig. 1.

Base isolation relies on a dynamic decoupling of the building from its foundation. The basic principle is often introduced by reference to the single-degree-of-freedom (SDOF) model, which represents the building as a rigid mass supported on some form of spring-damper element to represent the isolation bearings. As illustrated in Fig. 2, by considering the transmissibility of the system, that is, the ratio of the response amplitude of the mass to that of the imposed ground motion, the bearings may be seen to provide a degree of vibration isolation once the forcing frequency sufficiently exceeds the isolation (natural) frequency of the system.

The SDOF model remains useful as an introduction to the subject but is far too simplistic for making any useful predictions of isolation performance. In particular, it fails to represent the distribution of mass and stiffness within a building, and therefore the resulting dynamic behaviour of the building itself; and it fails to represent at least half of the system, namely, the building foundation and surrounding ground. The shortcomings of this model are at the heart of what makes base-isolation design such a challenge.

2. The development of base isolation

Although there is some evidence of vibration-isolated buildings being constructed in the 1930s [2], the first recognisable base-isolated building is Albany Court, a block of flats constructed over St James' Park Station, London, in 1965. Rubber-steel laminated bearings were used, based on technology developed from bridge bearings [3, 4]. Such elastomeric bearings represent one of the two main types of modern isolation bearing; the second is helical steel springs. Springs were first used to manage foundation subsidence [5] but their use for vibration isolation grew in the 1980s, with one of the first major applications in the UK being the Bridgewater Concert Hall, Manchester.

Base-isolation design has clearly benefitted from over 50 years' of engineering practice. In this time, many practical problems concerning the specification and design of base-isolation systems have been addressed and incorporated into established design practice, including settlement, fire proofing of the bearings, and designing lateral restraining measures. This period has also seen various developments in the bearings themselves, including synthetic rubber alternatives, dampers and 'noise stop pads' for spring bearings, and the development of pre-compressed bearings. Despite these developments, the governing theory and

Figure 1: Modern examples of base-isolated buildings include (a) an apartment block in Liverpool, UK, isolated from the city's underground railway on elastomeric bearings, and (b) a cinema beside Siegburg station, Germany, supported on steel springs. Images courtesy of CDM UK and GERB Schwingungsisolierungen.

fundamental understanding of isolation performance has been slow to keep pace, and there is a significant lack of formal guidance on all aspects of design. The only standard of direct relevance is the British Standard BS 6177 [6], which was formally withdrawn in 2013. This deals specifically with elastomeric bearings and is concerned principally with safety and practical aspects; no theoretical background or quantitative guidance is provided concerning the effectiveness of bearings as vibration isolators. The practicing engineer is therefore reliant on general guidance concerning noise and vibration in buildings, such as the American FTA guidelines [7], which cover the measurement and

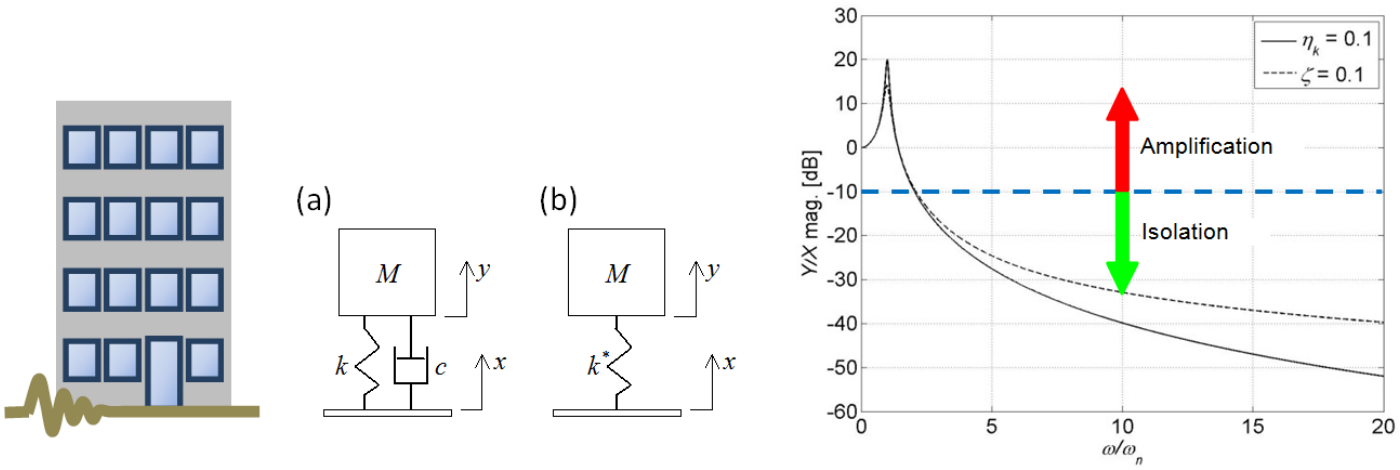

Figure 2: The SDOF model of a base-isolated building, where the rigid mass *M* represents the building and the linear spring *k* represents the isolation bearing. Damping may be accounted for by either (a) a viscous dashpot or (b) a complex (hysteretic) spring stiffness.

assessment of groundborne vibration but provide no specific guidance on base isolation.

The lack of guidance is a matter of significant concern for practicing engineers. There is a real need for an efficient, evidence-based design approach, based on robust engineering science, which leads to buildings of predictable vibration serviceability. Substantial progress has been made towards such a performance-based design approach within the field of seismic engineering, where the aim is to produce buildings of predictable seismic performance [8]. Work in Cambridge is aiming to make similar progress with base-isolation against groundborne vibration.

3. Design evaluation: the significance of complexity and uncertainty

The first step in the evaluation of any isolation design is to establish what vibration levels are likely to exist within the building with and without the isolation in place. This is far from straightforward, not least because the building structure is usually quite different in the two cases. Above all, it is the complexity and uncertainty of the underground environment that dominates the current uncertainty over how best to evaluate the performance of base isolation.

Complexity and uncertainty in the ground

In addition to the natural lithology, the urban underground environment contains many buried structures (services, foundations, tunnels, etc.), resulting in an often overwhelming complexity for the engineer concerned with groundborne vibration propagation. Modern numerical methods enable some of this complexity to be accounted for, in both source and foundation models [9, 10], but these are computationally expensive and remain research-oriented rather than design-oriented. In any case, as more complex models are developed, it becomes increasingly clear that the overriding concern is the uncertainty associated with the underground environment. The level of modelling uncertainty highlighted in a number of parametric and empirical studies [11–13] is highly significant, being comparable to the typical level of base-isolation performance believed to be achievable in practice.

Complexity and uncertainty in buildings

Unfortunately, although the influence of the ground tends to be the least well understood aspect in any base-isolation design, the building itself is not free from complex and uncertain behaviour. An example of current interest is the influence of non-structural elements of the building. Typical building models focus on the primary structure – the steel or concrete portal frame and its floors – where the natural approach is to use a commercial finite-element code, since these are readily available and often already employed in the structural (static) design. When using such models as the basis for a dynamic analysis, it is rare that consideration is given to non-structural elements, such as the exterior cladding and internal partitions. Recent work on the response of floors to human footfall suggests that this omission may be significant [14], and this raises questions over the significance of non-structural elements within the higher frequency range of groundborne vibration.

In summary, the complexity of the base-isolated building system, and the uncertainty associated with its response to groundborne vibration, are both highly significant for the practicing engineer attempting to evaluate isolation designs. Indeed, the value of deterministic modelling alone is clearly limited. Current models must be regarded as suitable for guiding design, by predicting the relative performance of different design options, rather than producing reliable predictions of absolute performance.

4. Towards a performance-based design approach

Further research is clearly required to develop generic methods for evaluating the performance of base-isolation systems.

The importance of measurements

To avoid the need to model the source and transmission path explicitly, and eliminate the associated modelling uncertainty, measurements should be used wherever possible to characterise the vibration at the proposed site of any building. Of course, measurements themselves are not without uncertainty, and care should be taken to ensure that these are as representative as possible of the 'input' seen by the building. Exactly where and what to measure are key questions [15], as is how to quantify the measurement uncertainty and the degree of correlation in vibration levels across a site.

The importance of soil-structure interaction

By far the most significant aspect of managing the complexity of the ground is accounting for soil-structure interaction (SSI); something that has only begun to be recognised relatively recently with the development of more comprehensive models. An outline deterministic approach to modelling base-isolation performance illustrates the point [16]. If it is attempted to predict vibration levels in a building without any reference to the ground or building foundation, two primary effects of SSI are neglected: (1) the radiation damping provided by the surrounding soil to the building structure; and (2) the modification of the free-field vibration by the constraining effect of the building. Both effects tend to reduce significantly the final vibration levels in the building [17, 18]. The incorporation of SSI into formalised design evaluation methods is therefore essential if models are not to over-predict final vibration levels and lead to inefficient designs.

The importance of an appropriate performance metric

It is common to refer to the performance of a base-isolation system in terms of insertion gain (IG), which is equivalent to the transmissibility of the equivalent SDOF system and compares the vibration amplitude(s) in the building in the isolated and un-isolated condition. However, being based on vibration amplitudes, IG varies with direction and position within a building, and it is unable to account sensibly for the various modes and paths of vibration transmission in a real building. Clearly, if an isolation design is to be evaluated properly, it is important to have a single performance metric. Power-flow insertion gain (PFIG) is one such metric, based on the mean vibrational power flowing into a building over a specified frequency band [15, 16]. Once a reliable model is established, PFIG is effective for guiding design because a reduction in this is guaranteed to reduce the average noise and vibration levels within a building. An additional benefit is the greater insight provided by power flow analysis, in general, than one based on vibration amplitude [19, 20]. See Fig. 3.

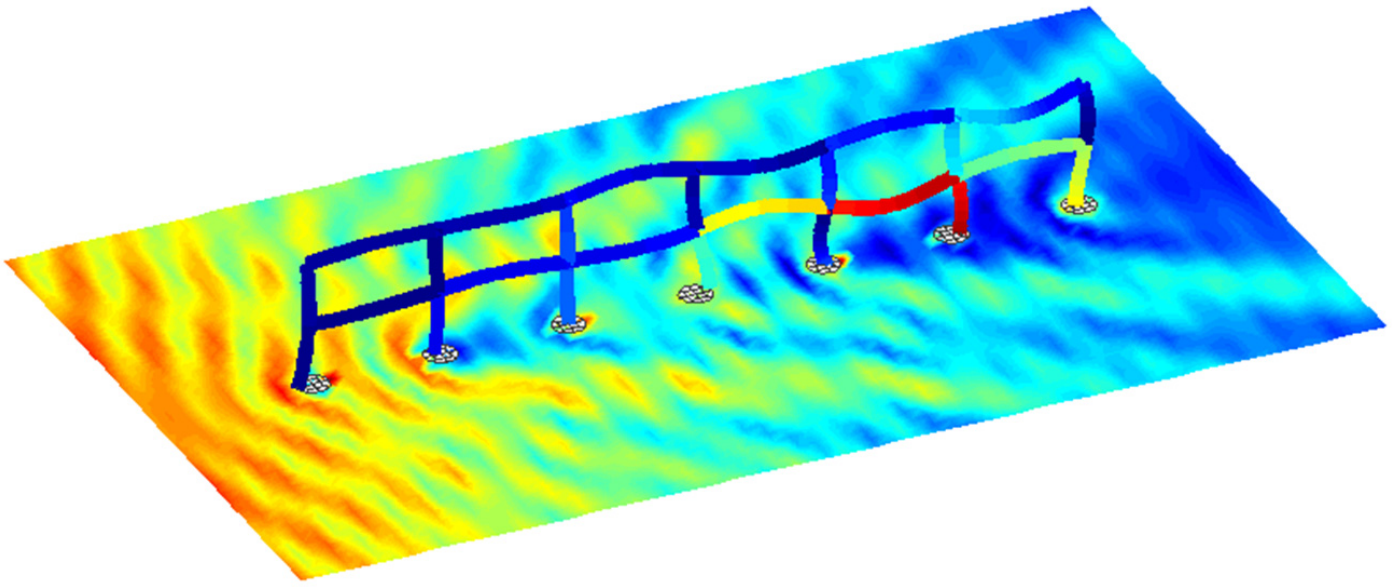

Figure 3: An example application of power flow analysis, investigating the dominant vibration transmission paths within a partially base-isolated building excited by surface Rayleigh waves.

5. Conclusions

Base-isolation against groundborne vibration has come a long way since it was first introduced over 50 years ago. Many practical problems concerning the specification and design of base-isolated buildings have been addressed, and such buildings are now commonplace in our major cities. Despite this, the governing theory and fundamental understanding of isolation performance remains lacking, and there is a real need for a performance-based design approach that enables practicing engineers to produce buildings of predictable isolation performance. The evaluation of isolation performance remains a significant challenge, primarily due to the complexity and uncertainty of the underground environment. Deterministic modelling alone provides only limited guidance. Modelling must be supplemented by measurements, wherever possible, and a thorough understanding of dynamic behaviour such as soil-structure interaction and the influence of non-structural building elements, which are rarely considered in current design practice. Such aspects remain key priorities of current research.

References

[1] Talbot, J. P. (2016). Building on springs: towards a performance-based design approach for controlling groundborne vibration. *Distinguished Plenary Lecture, ICSV23: 23rd International Congress on Sound and Vibration*, Athens, Greece.

[2] Waller, R. A. (1969). *Building on Springs*. Pergamon Press, Oxford, UK.

[3] Anon (1975). Long-term tests confirm laboratory predictions. *Rubber Developments,* **28:** 7–10.

[4] Waller, R. A (1966). A block of flats isolated from vibrations. *Environmental Engineering – Its Role in Society*, Symposium Paper No. 9, Society of Environmental Engineers, London.

[5] Huffmann, G. K. (1988). Spring support of buildings: a GERB system for full base isolation and for protection against subsidences. *American Society of Mechanical Engineers, Pressure Vessels and Piping Division*, **147:** 101–107.

[6] BS 6177 (1982). *Guide to selection and use of elastomeric bearings for vibration isolation of buildings*. BSI, London, UK.

[7] Hanson, C. E., Towers, D. A., & Meister, L. D. (2006). Transit Noise and Vibration Impact Assessment. *Report FTA-VA-90-1003-06*, U.S. Department of Transportation, Federal Transit Administration, Office of Planning and Environment.

[8] Ghobarah, A. (2001). Performance-based design in earthquake engineering: state of development. *Engineering Structures*, **23:** 878–884.

[9] Ntotsios, E., Hamad, W. I., Thompson, D. J., et al. (2015). Predictions of the dynamic response of piled foundations in a multi-layered halfspace due to inertial and railway induced loadings. *COMPDYN 2015: 5th International Conference on Computational Methods in Structural Dynamics and Earthquake Engineering*, Crete, Greece.

[10] Hamad, W. I., Ntotsios, E., Hunt, H. E. M., et al. (2015). Modelling the dynamic pile-soil-pile interaction in multi-layered half-space. *Euronoise 2015: 10th European Congress and Exposition on Noise Control Engineering*.

[11] Gupta, S., Stanus, Y., Lombaert, G., et al. (2009). Influence of tunnel and soil parameters on vibrations from underground railways. *Journal of Sound and Vibration*, **327:** 70–91.

[12] Gupta, S., Degrande, G., & Lombaert, G. (2009). Experimental validation of a numerical model for subway induced vibrations. *Journal of Sound and Vibration*, **321:** 786–812.

[13] Brookes, D., Hamad, W. I., Talbot, J. P., et al. (2016). On the dynamic interaction effects of railway tunnels: Crossrail and the Grand Central Recording Studios. *Proc. Institution of Mechanical Engineers Part F – Journal of Rail and Rapid Transit*, 1–18.

[14] Devin, A., Fanning, P. J. ,& Pavic, A. (2015). Modelling effect of non-structural partitions on floor modal properties. *Engineering Structures*, **91:** 58–69.

[15] Talbot, J. P., & Hunt, H. E. M. (2003). Isolation of buildings from rail-tunnel vibration: a review. *Building Acoustics*, **10:** 177–192.

[16] Talbot, J. P. (2007). Base isolation of buildings for control of ground-borne vibration, in *Handbook of Noise and Vibration Control*, Crocker, M. J., ed., John Wiley & Sons, Hoboken, NJ.

[17] Coulier, P., Lombaert, G., & Degrande, G. (2014). The influence of source-receiver interaction on the numerical prediction of railway induced vibrations. *Journal of Sound and Vibration*, **333:** 2520–2538.

[18] Talbot, J. P., Hamad, W. I., & Hunt, H. E. M. (2014). Base-isolated buildings and the added-mass effect. *International Conference on Noise and Vibration Engineering*, Leuven, Belgium.

[19] Heaton, M. J., & Talbot, J. P. A (2015). Power-flow based investigation into the performance of partial base-isolation for mitigating groundborne noise and vibration in buildings. *Proceedings of the 22nd International Congress on Sound and Vibration*, Florence, Italy.

[20] Sanitate, G., & Talbot, J. P. A (2016). Power-flow based investigation into the response of tall buildings to ground-borne vibration. *Proceedings of the 23rd International Congress on Sound and Vibration*, Athens, Greece.

Seismic Site Characterisation in Low Seismicity Regions

Sarah Tallett-Williams
Imperial College, London, UK.

Construction of new sensitive infrastructure is increasing the vulnerability of low seismicity regions to earthquake hazard, particularly new nuclear power facilities. However, probabilistic seismic hazard assessment (PSHA) of these regions has a large uncertainty due to the small catalogue of previous earthquake records (Edwards et al., 2008). If the site amplification associated with the strong ground motion station measurements is characterised, the model of this uncertainty can be improved, and parameters such as attenuation better constrained.

Site amplification from the local geology in the near surface can have a significant effect on built structures. However, it is challenging to characterise. The most effective, descriptive parameters are also expensive to measure in situ, principally shear wave velocity (V_s). In addition, Lemoine et al. (2012) showed that current proxy V_s methods, which aim to be used without in situ testing, are generally unsuitable outside the region for which they were defined. Therefore, in order to characterise large networks of many sites in low seismicity regions a new more economic method is required.

A total of 15 of the UK strong ground motion stations were investigated using desk studies, analysis of previous in situ tests and walk over surveys (Tallett-Williams et al., 2015). This information was used to form a geological profile for each station (Figure 1). However, the main challenge was to correlate these models with a V_s profile. Few in situ V_s tests that have been carried out in the UK are freely available for calibration.

Therefore, a Global V_s Database of over 9000 records was created (Campbell et al., 2016). This data consists only of direct in situ tests of V_s with a sufficient geological log and testing quality. Trends between geology and V_s were identified by the database, such as the importance of grain size in soils. Using these results, the geological profiles of

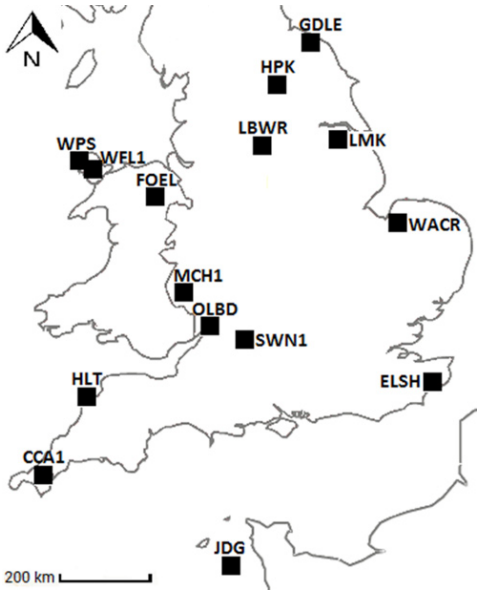

Figure 1: The 15 UK strong ground motion stations characterised during this study.

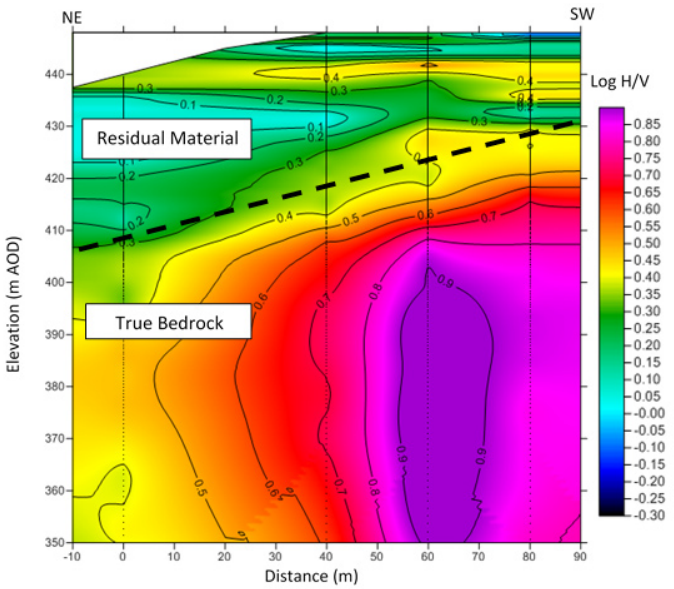

Figure 2: HSVR pseudo-seismic cross-section for an expected rock site, processed at 775 m/s with 0.25 exponent. Low H/V values in blue-green indicate low stiffness material, while red-purple indicate rock. Though due to the average processing speed the residual material appears deeper than likely in reality, the significant layer does allow for site amplification at the site.

the strong ground motion stations were correlated by geological facies with the Global V_s Database records to form a V_s profile. When combined with the geological profile in adapted Toro (1995) equations, this Site Specific proxy method produces a probability distribution of the time-averaged shear wave velocity of the top 30 m (V_{s30}) for each site.

This newly developed Site Specific method was validated using the Horizontal/Vertical Spectral Ratio (HVSR) method (Nakamura, 1989). This method is economical, but indeterminate and must not be interpreted without calibration to the local geology. Generally the most accurate parameter used is the depth of the first stratum.

All 15 stations were tested using HVSR. Over half the stations had V_{s30} results within 10% of the Site Specific method, with an average difference of 18%. This is 20% less than the standard proxy methods (Chiou et al., 2008).

The method also highlighted several stations where hard rock was expected but a residual rock layer was determined. This layer could cause site amplification, where it has not previously been considered (Figure 2).

This study aims to provide a characterisation method that is economic and accurate within defined ranges. The Site Specific method can be used as preliminary, inexpensive test for large networks which highlights any sites that require further exploratory testing.

Acknowledgements

The work was supervised by Peter Stafford, Imperial College London, and Clark Fenton, University of Canterbury. The author would also like to thank Mike Raines for his generous advice and wise instruction, Brian Baptie, John Laughlin and the BGS, Matthew Free, Arup, and Micromed S.P.A. for their kind guidance and profitable discussion. Access to the sites was gratefully accepted from Mr & Mrs Hill.

References

Campbell, N., Fenton, C., & Tallett-Williams, S. (2016). An investigation into the effects of material properties on shear wave velocity in rocks/soils. *5th International Conference on Geotechnical adn Geophysical Site Characterisation*, Queensland, Australia.

Chiou, B., Darragh, R., Gregor, N., & Silva, W. (2008). NGA project strong-motion database. *Earthq. Spectra*, **24:** 23–44.

Edwards, B., Rietbrock, A., Bommer, J. J., & Baptie, B. (2008). The acquisition of source, path, and site effects from microearthquake recordings using *Q* tomography: application to the United Kingdom. *Bull. Seismol. Soc. Am.,* **98:** 1915–1935.

Lemoine, A., Douglas, J., & Cotton, F. (2012). Testing the applicability of correlations between topographic slope and V_{s30} for Europe. *Bull. Seismol. Soc. Am.,* **102:** 2585–2599.

Nakamura, Y. (1989). Method for dynamic characteristics estimation of subsurface using microtremor on the ground surface. *Q. Rep. RTRI,* **30:** 25–33.

Tallett-Williams, S., Fenton, C., & Raines, M. (2015). Development of V_{s30} ground profiles for UK strong motion instrument sites. *16th European Conference on Soil Mechanics and Geotechnical Engineering*, Edinburgh, Scotland

Toro, G. R. (1995). Probabilistic models of site velocity profiles for generic and site-specific ground motion amplification studies In: Silva, W., Abrahamson, N., Toro, G., Costantino, C. (Eds.), *Description and Validation of the Stochastic Ground Motion Model. Pacific Engineering and Analysis*, Brookhaven Library, Upton, New York, 1030–1176.

Notable Earthquakes January 2016 – December 2016

Reported by British Geological Survey

Issued by: Davie Galloway, British Geological Survey, December 2016 and April 2017.
Non British Earthquake Data supplied by The United States Geological Survey.

Year	Day	Mon	Time UTC	Lat	Lon	Dep km	Magnitude ML	Mb	Mw	Location
2016	03	JAN	23:05	24.80N	93.65E	55			6.7	MANIPUR, NE INDIA
At least eleven people killed (six in India and another five in Bangladesh), over 200 others injured and a large number of buildings damaged in the state of Manipur.										
2016	07	JAN	18:52	53.09N	5.15W	11	1.8			IRISH SEA
2016	07	JAN	22:03	51.28N	0.51E	3	1.6			MAIDSTONE, KENT
2016	11	JAN	16:38	3.90N	126.86E	13			6.5	TALLAUD, INDONESIA
2016	14	JAN	03:25	41.97N	142.78E	46			6.7	HOKKAIDO, JAPAN
2016	20	JAN	18:59	58.89N	1.42E	8	2.3			NORTHERN NORTH SEA
2016	21	JAN	18:06	18.82N	106.93W	10			6.6	JALISCO, MEXICO
2016	21	JAN	18:51	59.17N	1.97E	12	1.9			NORTHERN NORTH SEA
2016	24	JAN	10:30	59.64N	153.41W	129			7.1	SOUTHERN ALASKA
2016	25	JAN	04:22	35.65N	3.68W	12			6.3	STRAIT OF GIBRALTAR
One person was killed (from a heart attack) in Al Hoceima, Morocco. Many buildings in Nador suffered from minor damage and at least 26 people were injured and several buildings were damaged in the Spanish autonomous city of Melilla.										
2016	27	JAN	23:28	50.16N	5.12W	2	0.8			PENRYN, CORNWALL
Felt Rame (2 EMS)										
2016	30	JAN	03:25	53.98N	158.55E	177			7.2	KAMCHATKA, RUSSIA
2016	05	FEB	19:57	22.94N	120.60E	23			6.4	TAIWAN
At least 117 people were killed from the collapse of the Wijuan Jinlong apartment building and over 525 others were injured in Tainan.										
2016	15	FEB	23:12	49.90N	3.11W	5	1.6			ENGLISH CHANNEL
2016	25	FEB	12:26	51.50N	2.90E	9	2.7			SOUTHERN NORTH SEA
2016	25	FEB	22:08	58.78N	1.42E	10	2.4			NORTHERN NORTH SEA
2016	02	MAR	12:49	4.95S	94.33E	24			7.8	SUMATRA, INDONESIA
2016	05	MAR	04:16	53.37N	2.36E	5	2.4			SOUTHERN NORTH SEA
2016	06	MAR	23:12	51.72N	0.94W	3	2.3			THAME, OXFORDSHIRE
2016	07	MAR	05:40	61.56N	3.84E	10	2.9			NORTHERN NORTH SEA
2016	07	MAR	20:11	58.41N	1.11E	6	2.4			NORTHERN NORTH SEA
2016	11	MAR	20:30	52.69N	0.72W	3	1.0			OAKHAM, RUTLAND
Felt Oakham (2 EMS).										
2016	14	MAR	18:06	52.68N	0.76W	3	1.0			OAKHAM, RUTLAND
Felt Oakham (2 EMS).										
2016	03	APR	08:23	14.32S	166.86E	26			6.9	VANUATU
2016	06	APR	06:58	14.07S	166.63E	24			6.7	VANUATU
2016	07	APR	03:32	13.98S	166.59E	27			6.7	VANUATU
2016	10	APR	10:28	36.47N	71.13E	212			6.6	HINDU KUSH, AFGHANISTAN
Six people killed, several others injured and many homes heavily damaged in Khyber Pakhtunkhwa and in Gilgit, Pakistan.										

Year	Day	Mon	Time UTC	Lat	Lon	Dep km	Magnitude ML	Mb	Mw	Location
2016	13	APR	13:11	49.42N	2.50W	9	1.6			GUERNSEY, CHANNEL ISLES
Felt Guernsey (2 EMS).										
2016	13	APR	13:55	23.09N	94.87E	136			6.9	MYANMAR
Two people killed, 70 others injured and several buildings damaged in Assam, India and at least 100 others were injured in the Chittagong, Dhaka and Sylhet areas of Bangladesh.										
2016	13	APR	22:01	54.75N	3.64W	6	1.7			SOLWAY FIRTH
2016	14	APR	12:26	32.79N	130.70E	9			6.2	KYUSHU, JAPAN
At least nine people were killed, over 1,000 others were injured and many homes were destroyed or severely damaged in Kumamoto Prefecture.										
2016	15	APR	16:25	32.79N	130.75E	10			7.0	KYUSHU, JAPAN
At least 40 people killed, another 2,000 plus injured and over 12,500 houses and 445 public buildings were damaged or destroyed in Kumamoto and Oita Prefectures. The Kyushu Shinkansen train service was suspended after a train derailed. Many power outages occurred and widespread damage was caused to roads, bridges, tunnels and water lines throughout the region. Damage has been estimated at US$12 billion.										
2016	15	APR	18:26	62.05N	2.19E	10	2.8			NORWEGIAN SEA
2016	16	APR	23:58	0.38N	79.92W	20			7.8	ECUADOR
At least 668 killed (with nine still missing), over 27,700 injured and over 7,000 buildings destroyed including most of the town of Pedernales and its surrounding urban areas. Several landslides occurred and many roads and power lines were damaged. A tsunami was also generated with a maximum wave height of 25 cm recorded on a tide gauge offshore Esmeraldas, Ecuador.										
2016	18	APR	20:49	51.97N	2.75W	4	1.7			HEREFORD, HEREFORDSHIRE
Felt Much Dewchurch and Little Dewchurch (2 EMS).										
2016	21	APR	01:22	58.93N	1.46E	18	2.1			NORTHERN NORTH SEA
2016	25	APR	01:25	59.87N	0.41E	5	1.8			NORTHERN NORTH SEA
2016	28	APR	19:33	16.04S	167.38E	24			7.0	VANUATU
2016	29	APR	01:33	10.28N	103.74W	10			6.6	NORTHERN EAST PACIFIC RISE
2016	09	MAY	11:25	56.67N	4.38W	3	1.3			FINNART, PERTH & KINROSS
Felt Dall (2 EMS).										
2016	15	MAY	17:31	59.81N	2.45E	10	2.3			NORTHERN NORTH SEA
2016	17	MAY	15:56	56.16N	4.93W	9	1.9			LOCH GOIL, ARGYLL & BUTE
Felt Lochgoilhead (2 EMS).										
2016	18	MAY	07:57	0.43N	79.79W	16			6.7	ECUADOR
2016	18	MAY	16:46	0.50N	79.62W	30			6.9	ECUADOR
One person killed and 87 others injured in Manabi Province. Several buildings heavily damaged in Esmeralda and Portoviejo.										
2016	18	MAY	23:00	56.39N	5.48W	4	1.9			OBAN, ARGYLL & BUTE
Felt Oban, Connel, North Connel, Knipoch, Glencruitten, Benderloch, Kilmelford, Taynuilt, Dunbeg, Kilmore and Ardchattan (3 EMS).										
2016	26	MAY	19:55	64.40N	4.22W	10	3.3			NORWEGIAN SEA
2016	28	MAY	05:38	21.97S	178.20W	405			6.9	FIJI ISLANDS REGION
2016	28	MAY	09:46	56.24S	26.94W	78			7.2	SOUTH SANDWICH ISLANDS
2016	30	MAY	04:10	57.68N	5.65W	7	1.3			SHIELDAIG, HIGHLAND
Felt Gairloch (2 EMS).										
2016	01	JUN	22:56	2.10S	100.67E	50			6.6	SUMATRA, INDONESIA
At least 30 people injured and around 900 buildings damaged in Bengkulu and West Sumatera Provinces.										
2016	04	JUN	13:22	60.74N	2.20E	19	2.8			NORTHERN NORTH SEA

Year	Day	Mon	Time UTC	Lat	Lon	Dep km	Magnitude ML	Mb	Mw	Location
2016	13	JUN	21:40	53.24N	3.74W	8	1.9			COLWYN BAY, CONWY
Felt Colwyn Bay, Betws-y-Coed and in the Conwy Valley (Conwy), in Bangor, Llanberis, Caernarfon, Bethesda, Tregarth, Rhosgadfan and LLanllechid (Gwynedd) and in Llanfairpwllgwynyll and Menai Bridge (Isle of Anglesey) (3 EMS).										
2016	22	JUN	17:26	56.29N	5.86W	3	1.2			MULL, ARGYLL & BUTE
Felt Mull (2 EMS).										
2016	24	JUN	22:22	59.75N	1.78E	10	2.3			NORTHERN NORTH SEA
2016	29	JUN	20:58	53.51N	2.17W	3	1.4			MIDDLETON, GTR MANCHESTER
Felt Middleton (2 EMS).										
2016	29	JUL	21:18	18.54N	145.51E	196			7.7	MARIANA ISLANDS
2016	12	AUG	01:26	22.48S	173.12E	16			7.2	LOYALTY ISLANDS
2016	15	AUG	0259	15.65S	72.01W	20			5.5	SOUTHERN PERU
Nine people killed, at least 68 others injured and around 1,250 houses/buildings either destroyed or damaged (including eight churches and fifteen schools) in Achoma, Yanque and Caylloma.										
2016	19	AUG	07:32	55.29S	31.88W	10			7.4	SOUTH GEORGIA ISLAND
2016	19	AUG	13:38	56.39N	5.85W	2	1.9			MULL, ARGYLL & BUTE
Felt Mull (3 EMS).										
2016	24	AUG	01:36	42.72N	13.19E	4			6.2	UMBRIA, ITALY
At least 297 people killed, 400 others injured and widespread damage occurred in the Arquata del Tronto, Accumoli and Amatrice regions.										
2016	24	AUG	10:34	20.92N	94.57E	82			6.8	MYANMAR
Four people killed and more than 230 buildings damaged in the epicentral region. Several ancient monuments were also damaged in the Bagan area.										
2016	29	AUG	04:29	0.05S	17.83W	10			7.1	SOUTH ATLANTIC OCEAN
2016	31	AUG	19:38	50.12N	0.38W	7	1.9			ENGLISH CHANNEL
2016	31	AUG	03:11	3.69S	152.79E	476			6.8	PAPUA NEW GUINEA
2016	01	SEP	16:37	37.36S	179.15E	19			7.0	NEW ZEALAND
2016	09	SEP	22:00	61.07N	3.57W	10	3.9			NORWEGIAN SEA
2016	10	SEP	12:27	1.04S	31.62E	40			5.9	TANZANIA
At least nineteen people killed, 253 injured and over 2,000 houses destroyed or severely damaged in Bukoba, Tanzania. A further four people were killed and another seven were injured in Kamuli and Rakai, Uganda.										
2016	23	SEP	16:11	2.65S	29.06E	10		4.8		BURUNDI
At least seven people killed, several more injured and many buildings damaged in Bukavu, Congo and another person killed and twenty others injured in Rusizi, Rwanda.										
2016	24	SEP	21:28	19.78S	178.24W	596			6.9	FIJI ISLANDS REGION
2016	09	OCT	12:48	62.49N	2.18W	28	3.8			NORWEGIAN SEA
2016	17	OCT	06:14	6.00S	148.89E	42			6.8	PAPUA NEW GUINEA
2016	19	OCT	00:26	4.86S	108.16E	614			6.6	JAVA SEA, INDONESIA
2016	27	OCT	02:08	50.51N	4.53W	11	2.3			LISKEARD, CORNWALL
Felt Liskeard, Bodmin, St Breward, Doublebois, Polperro, Treveighan, Henwood, Lanreath, Haynes, St Maybn, St Teath, Par, Helstone, Wadebridge, St Columb Major, Lostweithel, Altarnun, St Neot, Redmoor, Golderdon, St Minver, North Hill, Camelford, Calstock, Delabole, St Wenn and Newquay, Cornwall (3EMS).										
2016	29	OCT	19:20	59.99N	2.30W	10	2.4			NORTHERN NORTH SEA
2016	30	OCT	06:40	42.86N	13.10E	8			6.6	UMBRIA, ITALY
Two people killed, twenty others injured and further serious damage occurred in the Arquata del Tronto, Accumoli and Amatrice regions.										

Year	Day	Mon	Time UTC	Lat	Lon	Dep km	Magnitude ML	Mb	Mw	Location
2016	02	NOV	03:51	49.53N	4.39W	4	2.0			ENGLISH CHANNEL
2016	03	NOV	10:57	58.74N	1.63W	23	3.9			NORTHERN NORTH SEA
2016	03	NOV	14:19	57.26N	4.75W	4	1.7			INVERMORISTON, HIGHLAND
2016	07	NOV	02:02	53.01N	2.20W	10	2.1			SOUTHERN NORTH SEA
2016	13	NOV	11:02	42.74S	173.05E	15			7.8	NEW ZEALAND
One person killed in Kaikoura and one person killed in Mount Lyford. Widespread damage to buildings and docks and many power outages occurred in Wellington. A tsunami was generated as a result of the earthquake, which was recorded on several tide gauges in the region. Surface faulting was observed on some faults, with a maximum uplift of about 10 metres and about 110 km of coastal uplift was observed in Marlborough and northern Canterbury.										
2016	13	NOV	11:32	42.32S	173.67E	10			6.5	NEW ZEALAND
2016	14	NOV	00:34	42.61S	173.25E	9			6.5	NEW ZEALAND
2016	14	NOV	07:20	51.89N	3.17W	5	2.1			CRICKHOWELL, POWYS
2016	21	NOV	20:59	37.39N	141.39E	9			6.9	OFFSHORE HONSHU, JAPAN
Fifteen people injured and minor damage occurred in Fukushima and a tsunami with a maximum wave height of 1.4 metres was recorded at Sendai.										
2016	24	NOV	18:43	11.91N	88.90W	10			6.9	OFFSHORE EL SALVADOR
2016	25	NOV	14:24	39.27N	73.98E	17			6.6	SW XINJIANG, CHINA
2016	06	DEC	22:03	5.28N	96.17E	13			6.5	NORTH SUMATRA, INDONESIA
At least 104 people killed, over 1,270 injured and at least 18,752 buildings destroyed or damaged in Aceh.										
2016	08	DEC	14:49	40.45N	126.19W	8			6.6	OFFSHORE CALIFORNIA
2016	08	DEC	17:38	10.68S	161.33E	40			7.8	SOLOMON ISLANDS
2016	08	DEC	21:56	10.84S	161.31E	12			6.5	SOLOMON ISLANDS
2016	09	DEC	19:10	10.75S	161.13E	19			6.9	SOLOMON ISLANDS
2016	10	DEC	01:22	51.80N	4.03W	11	1.9			SARON, CARMARTHENSHIRE
2016	13	DEC	02:06	55.06N	3.65W	12	2.1			SOUTHERN NORTH SEA
2016	13	DEC	14:58	58.19N	0.84W	14	2.4			NORTHERN NORTH SEA
2016	17	DEC	10:51	4.51S	153.52E	94			7.9	PAPUA NEW GUINEA
2016	19	DEC	07:11	0.86N	79.71W	10			5.4	ECUADOR
Three people killed, 47 others injured, ten homes destroyed and 70 others damaged in Esmeraldas.										
2016	21	DEC	00:17	7.51S	127.92E	152			6.7	BANDA SEA, INDONESIA
2016	21	DEC	17:10	58.22N	0.99W	11	1.8			NORTHERN NORTH SEA
2016	25	DEC	14:22	43.41S	73.94W	38			7.6	CHILOE ISLAND, CHILE

SECED Newsletter

The SECED Newsletter is published quarterly. All contributions of relevance to the members of the Society are welcome. Manuscripts should be sent by email. Diagrams, pictures and text should be attached in separate electronic files. Hand-drawn diagrams should be scanned in high resolution so as to be suitable for digital reproduction. Photographs should likewise be submitted in high resolution. Colour images are welcome.

Please contact the Editor of the Newsletter, Damian Grant, for further details: damian.grant@arup.com.